1.3-μm Reflection Insensitive InAs/GaAs Quantum Dot Lasers Directly Grown on Silicon

Jianan Duan, *Student Member, IEEE*, Heming Huang, Bozhang Dong, Daehwan Jung, Justin C. Norman, John E. Bowers, *Fellow, IEEE*, and Frédéric Grillot, *Senior Member, IEEE*

***Abstract*— This letter reports on a 1.3-μm reflection insensitive transmission with a quantum dot laser directly grown on silicon in the presence of strong optical feedback. These results show a penalty-free transmission at 10 GHz under external modulation with −7.4-dB optical feedback. The feedback insensitivity results from the low linewidth enhancement factor, the high damping, the absence of off-resonance emission states, and the shorter carrier lifetime. This letter paves the way for future on chip high-speed integrated circuits operating without optical isolators.**

***Index Terms*— Semiconductor lasers, quantum dots, photonics integrated circuits, optical feedback.**

I. Introduction

SILICON photonics is important for high-speed telecom and datacom optical systems as well as future optical interconnects, board-to-board and chip-to-chip integrated photonics [1], [2]. Silicon (Si) is a very efficient semiconductor material for waveguiding light owing to the strong index contrast with silica. However, the indirect band gap nature makes the realization of light emitters from Si highly inefficient with extremely poor radiative efficiency meaning that other techniques such as wafer-bonding must be investigated if light emission is to be realized [3]. Most lasers are relatively sensitive to optical reflections hence still necessitating the inclusion of an expensive optical isolator. Such hybrid semiconductor lasers made with several passive and active interfaces/transitions between the III-V material and Si suffer from multiple internal reflections which when combined with external ones can become highly problematic for the laser stability [4]. As no on-chip optical isolators and circulators integrated with lasers and having sufficient isolation ratio exist, development of feedback insensitive transmitters remains a major objective that can revolutionize the core technology of the physical layer. In this context, InAs/GaAs quantum dot (QD) lasers using nanostructures as gain media display a strong potential for cost reduction [5]. For instance, a recent work has reported on an InAs/GaAs QD laser transmitter integrated on Si substrate without optical isolator for core I/O applications. An error-free transmission was successfully demonstrated at 25 Gbps using a pseudo random binary sequence (PRBS) pattern of $2^7 - 1$ [6]. Overall, QD lasers are more stable against optical feedback as opposed to their bulk or quantum well (QW) counterparts because of their quasi-class A behavior originated from the large damping [7]. The critical feedback level associated to the undamping of the relaxation oscillations and leading to the so-called chaotic state (e.g. coherence collapse) usually takes place at a higher feedback level [8]. Although prior works showed that this large feedback resistance depends on the type of QDs [7], [9] and the carrier dynamics through for instance the doping concentration [10], no study has really reported on a total insensitivity down to a testbed environment. Such a difficulty can be explained as follows. In QD lasers, the impact of off-resonance energy states play an important role in the laser dynamics. In particular, prior research showed that a QD laser lasing on the sole ground state (GS) transition does not exhibit the same dynamical response under optical excitation as that emitting exclusively on the first excited state (ES) assuming that the two lasers were made with the same materials and come from the same wafer [11]. More recently, it was also proved that for a QD laser exhibiting the two transitions with respect to the bias current, the critical feedback level strongly depends on the ES-to-GS lasing threshold ratio meaning that a laser having a fast switching dynamics from GS to ES is more subject to be highly destabilized by parasitic reflections [12]. Among other advantages, QD lasers enable smaller devices, amplification, thermal stability, and a near zero linewidth enhancement factor (α_H-factor) as recently shown in an InAs/GaAs QD laser directly grown on Si [13]. This last feature is also of paramount importance for reflection insensitive applications since the feedback instabilities are fundamentally driven by the phase-amplitude coupling through the α_H-factor hence the smaller the α_H, the better stability against optical feedback.

Manuscript received October 25, 2018; revised January 17, 2019; accepted January 20, 2019. Date of publication January 25, 2019; date of current version February 13, 2019. This work was supported in part by the Advanced Research Projects Agency-Energy under Grant DE-AR000067 and in part the Institut Mines-Télécom. *(Corresponding author: Frédéric Grillot).*

J. Duan, H. Huang, and B. Dong are with LTCI, Télécom ParisTech, Université Paris-Saclay, 75013 Paris, France.

D. Jung was with the Materials Department, Institute for Energy Efficiency, University of California at Santa Barbara, Santa Barbara, CA 93106 USA. He is now with the Center for Opto-Electronic Materials and Devices, Korea Institute of Science and Technology, Seoul 02792, South Korea.

J. C. Norman is with the Materials Department, Institute for Energy Efficiency, University of California at Santa Barbara, Santa Barbara, CA 93106 USA.

J. E. Bowers is with the Materials Department, Institute for Energy Efficiency, University of California at Santa Barbara, Santa Barbara, CA 93106 USA, and also with the Department of Electrical and Computer Engineering, University of California at Santa Barbara, Santa Barbara, CA 93106 USA.

F. Grillot is with the Center for High Technology Materials, University of New Mexico, Albuquerque, NM 87106 USA, and also with LTCI, Télécom ParisTech, Université Paris-Saclay, 75013 Paris, France (e-mail: grillot@telecom-paristech.fr).

Color versions of one or more of the figures in this letter are available online at http://ieeexplore.ieee.org.

Digital Object Identifier 10.1109/LPT.2019.2895049

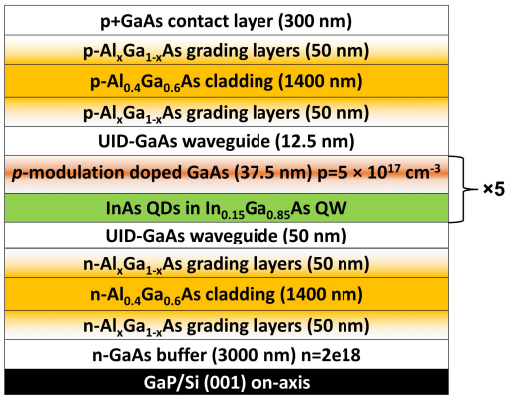

Fig. 1. Epi-structure of the InAs/GaAs QD laser on Si.

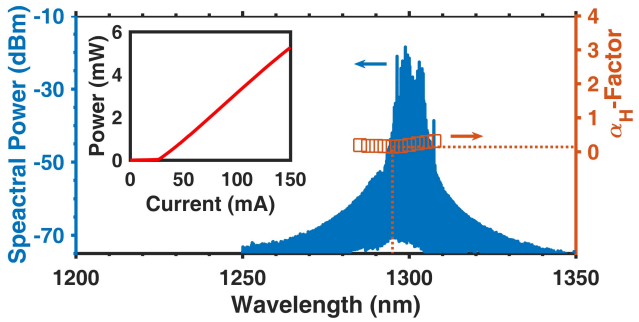

Fig. 2. Measured optical spectrum (blue) at $3 \times I_{th,GS}$ and extracted α_H-factor (orange) of the QD laser on Si. The inset represents the light-current characteristics of the laser at 20 °C.

In this letter, we report on a 1.3-μm reflection insensitive transmission with a Fabry-Perot (FP) QD laser directly grown on Si and operating under strong optical feedback. Although directly grown on Si, InAs/GaAs QD lasers operating on the GS transition exhibit low threshold current density, high thermal stability and reduced sensitivity to threading defects [1] which are in favor of the reduction of both production-cost and energy consumption. The results show that an error-free transmission at 10 GHz external modulation is obtained with 100% (i.e. −7.4 dB) optical feedback. Such a remarkable feedback insensitivity directly results from the low α_H-factor, the absence of ES emission, the large damping, and a shorter carrier lifetime. This work sheds light on novel reflection insensitive optical sources on Si with QD solutions, which are very promising for integrated photonics technologies.

II. Laser Structure and Experimental Apparatus

A representation of the epi-structure of the QD laser under study is presented in Fig. 1. The InAs/GaAs FP laser is 1.35 mm long with a 3.5 μm wide ridge waveguide. The active region contains 5 InAs dot layers directly grown on an on-axis (001) Si wafer in a Veeco Gen-II molecular beam epitaxy chamber, details on the growth process can be found elsewhere [14]. The full-width at half-maximum (FWHM) of the photoluminescence response is about 30 meV (not shown here), indicating that highly uniform QDs are obtained. The cavity facets are unevenly coated, with power reflectivity of 60% and 99% on the front and rear, respectively.

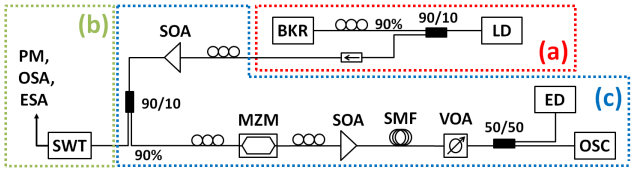

Fig. 3. Schematic of the experimental setup. Part (a): feedback laser source; part (b): monitoring the optical feedback sensitivity of the laser in terms of power and spectra; part (c): transmission performance test.

The room-temperature (20 °C) light-current characteristic curve is shown in the inset of Fig. 2 and the GS threshold current $I_{th,GS}$ is about 26.5 mA. The spectral distribution of the α_H-factor is illustrated in Fig. 2 (orange), exhibiting a minimum value of 0.13 at the GS transition gain peak of 1295 nm (dashed line) [13]. The optical spectrum (blue) is taken at $3 \times I_{th,GS}$, where the laser operates on the sole GS transition meaning that the ES transition does not show up with the increase of the bias current. In other words, this QD laser on Si exhibits a very large ES-to-GS lasing threshold ratio which is a figure of merit for maintaining a high degree of stability [12]. In order to properly probe the advantages of the QD laser on Si, a commercial QW FP laser is also used as a reference laser. The room-temperature threshold of the QW laser is at 28 mA, while the gain peak wavelength is centered at 1541 nm, with a corresponding α_H-factor of about 2.8.

Fig. 3 depicts the experimental setup used for the optical feedback experiment that consists of three parts. First in part (a), the emission from the laser diode (LD) is coupled through an anti-reflection (AR) coated lens-end fiber and divided into two paths, feedback path and output path. On the feedback path, 90% coupled power is directed to the backreflector (BKR) that consists of a mirror and a variable optical attenuator (VOA). The feedback strength r_{ext}, defined as the ratio between the returned power and the free-space emitted power at the coupling facet, is controlled and varied from 0% up to 100% (-7.4 dB). The losses from the fiber coupling and in the fiber setup are taken into account to accurately calculate r_{ext}, for which, the uncertainty is less than 0.1%. A polarization controller is inserted in the feedback path to compensate the fiber dispersion in the external cavity and to maximize the effects of the optical feedback namely to have the reflected light in the transverse electric (TE) polarization. The external cavity frequency is 14 MHz which corresponds to an external cavity length of 7 meters. This long delay configuration signifies that the ratio between the frequency of the external cavity f_{ext} and the laser's relaxation oscillation frequency f_{RO} is below one. Even though a photonic integrated circuit does not experience such long delay optical reflections, this configuration is studied here because it corresponds to the most stringent feedback conditions for the laser. In other words, using a long delay is more pertinent to fully evaluate the potential of the QD laser on Si against parasitic reflections. Finally, the other 10% of the coupled power is isolated and directed to the output path for further studies. Overall, this part is configured as a feedback QD laser source; In part (b), an optical switch (SWT) is installed at the input to redirect the light to the power meter (PM), optical

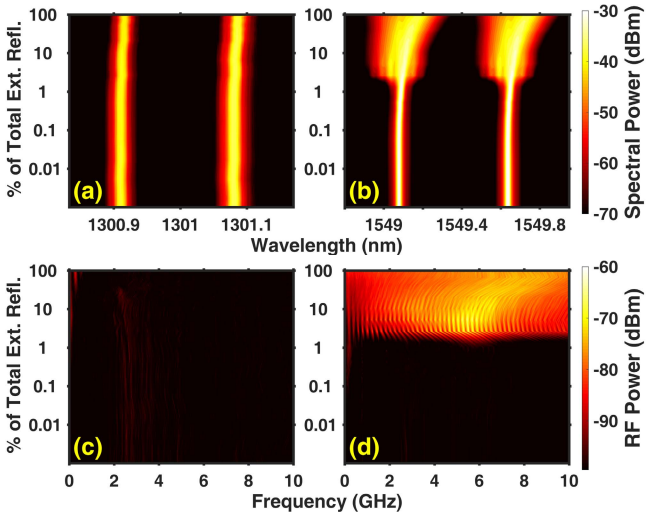

Fig. 4. (a) Optical and (c) RF spectral mappings of the QD laser on Si as a function of the feedback strength at $3 \times I_{th}$; (b) Optical and (d) RF spectral mappings of the QW laser as a function of the feedback strength at $3 \times I_{th}$. The vertical axis is in logarithmic scale.

and radio-frequency (RF) spectrum analyzer (OSA and ESA). The role of this part is to monitor the steadiness of the laser; The last part (c) is configured for the testbed experiment of the QD laser on Si operating with optical feedback. The power from part (a) output is amplified by a semiconductor optical amplifier (SOA), and then divided by a 90/10 fiber coupler. The 10% is sent to part (b) for monitoring, while the rest of 90% is guided to a Mach-Zehnder modulator (MZM). The modulation format is 10 GHz non-return-to-zero (NRZ) PRBS with a sequence length of $2^{31} - 1$ and the peak-to-peak modulation amplitude V_{pp} is 2V. The output from the MZM is again amplified and injected into a 2 km single-mode fiber (SMF) coil. Alternatively, when it comes to the case of the QW laser, the SOAs are replaced with Erbium-doped fiber amplifiers (EDFA), and the emission is filtered with a bandpass filter of 13 nm before being injected into the MZM. In the end, an error detector (ED) is connected to characterize the bit error rate (BER) and hence the transmission performance. In addition, a high-speed oscilloscope is also used for capturing the eye-diagram.

III. Static Response Under Optical Feedback

In this section, we focus on the laser's static response under optical feedback. To do so, part (a) is directly connected to part (b). Fig. 4 depicts the spectral evolution of both QD and QW lasers along with the increase of r_{ext} at $3 \times I_{th}$. The first row shows the mapping in the optical domain whereas the second is the RF one. As shown in Fig. 4(a), the QD laser on Si demonstrates a remarkable stability against optical feedback whatever the feedback strength. Only a slight red-shift of the modal wavelength is observed while the RF response in Fig. 4(c) does not show any sign of nonlinear oscillations. At this stage, the laser displays a chaos-free operation meaning that the coherence collapse state taking place beyond the critical feedback level does not show up in the range of feedback level considered in the experiment. Note that this statement remains perfectly valid even at $6 \times I_{th}$. Compared to [8], the QD lasers on Si used in this letter exhibit a stronger stability against optical feedback not only because the experiment is performed under the long delay condition but also because devices under study have a shorter cavity length and a much lower front facet reflectivity which can both contribute to strongly degraded feedback tolerance.

As for the QW laser, the device is not disturbed until 1.7% (i.e. -25 dB) which corresponds to the critical level associated to the onset of the undamping of the relaxation oscillations. A critical feedback level of -25 dB is similar to prior observations made with QW lasers [15]. At higher feedback levels, the laser starts experiencing the route to chaos through coherence collapse with strong broadening of the FP modes (Fig. 4(b)) and intense chaotic oscillations in the RF domain (Fig. 4(d)). Any further increase of the feedback strength leads to a more complex chaos (i.e. fully developed coherence collapse) then to a restablization [16]. In this work, these regimes were not all observed due to the induced loss in the long delay experiment.

In what follows, testbed experiments are performed so as to highlight the effects of the feedback insensitivity on a transmission system. To do so, external modulation of light is preferred since using direct modulation results in adding another degree of freedom to the laser. As a consequence of that, the phase-space dynamics becomes different such as the laser's dynamics and the critical feedback level, meaning that it is not possible to properly investigate the effects of the static optical feedback on the transmission performance.

IV. Dynamic Response Under Optical Feedback

The laser's dynamic response under optical feedback is studied at $3 \times I_{th}$. Fig. 5(a) shows the BER of the QD laser on Si with and without feedback for the back-to-back (B2B) configuration and after 2 km fiber transmission. For each B2B and transmission datasets, a perfect overlap between the BER plots is obtained for the solitary case and the case with optical feedback. Thus, the stability of the QD laser on Si is totally preserved up to a maximal optical feedback strength as large as $r_{ext} = 100\%$ (i.e. -7.4 dB) which is already much larger than any other typical reflection levels present in a transmission system. This large feedback resistance is higher than the tolerance level previously reported on GaAs-based QD lasers [11], and is very promising for the concept of reflection insensitive on-chip optical transmitters. Taking advantage of the chaos-free operation depicted in Fig. 4(c), the QD laser exhibits a penalty-free operation for BER $< 10^{-12}$. The wide open eye diagram shown in Fig. 5(b) confirms this tendency. After the transmission, the BER plots reveal a power penalty of 2 dB for a BER of 10^{-9}. However, it is important to stress that the penalty does not result from the optical feedback but it is rather attributed to the fiber dispersion and the amplified spontaneous emission induced noise from the SOA. The latter slightly degrades the eye-diagram (Fig. 5(c)) because of the residual mismatch between the laser operating wavelength (1301 nm, see in Fig. 2) and the SOA gain peak (1310 nm).

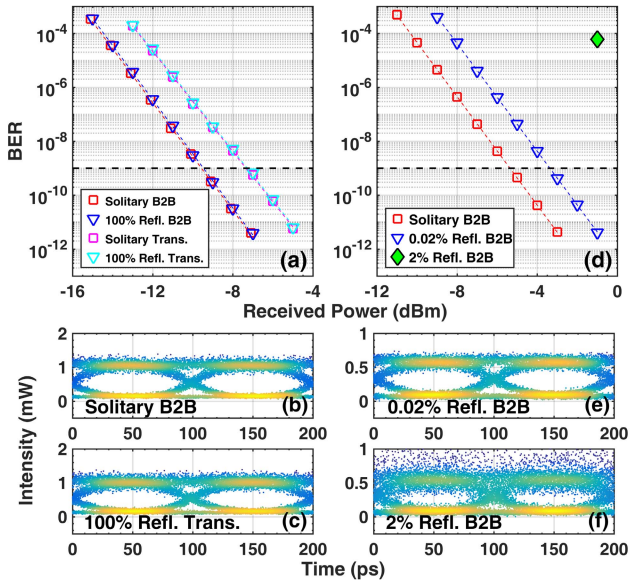

Fig. 5. (a) BER plots for: solitary QD laser in the back-to-back configuration (red, eye-diagram in (b)), QD laser with 100% optical feedback in the back-to-back configuration (blue), solitary QD laser after transmission (magenta), QD laser with 100% optical feedback after transmission (cyan, eye-diagram in (c)); (d) back-to-back BER curves for QW laser in free-running (red) and under 0.02% feedback (blue, eye-diagram in (e)). (f) eye-diagram of the laser under 2% feedback, above the critical level.

Despite that, the laser still achieves penalty-free operation for BER $< 10^{-12}$ between the solitary case and the case with optical feedback.

Similar experiments are then performed for the QW laser. The corresponding BER plots are displayed in Fig. 5(d) only for the B2B configuration. Biasing the laser in the stable regime e.g. below the critical feedback level (see in Fig. 4(b)) with $r_{ext} = 0.02\%$ (i.e. -44 dB), the transmission performance is found already affected with a 2 dB power penalty at BER$= 10^{-9}$, despite that the eye-diagram remains opened (Fig. 5(e)). Above the critical feedback level ($r_{ext} = 1.7\%$), the transmission performance is drastically degraded as shown in Fig. 5(f). Thus, for $r_{ext} = 2\%$ (i.e. -24 dB), the laser operates in the coherence collapse regime in which the data transmission is no longer possible as also confirmed by the noisy eye diagram [15]. The corresponding BER value is measured at 6×10^{-5} for a received power of -1 dBm (green diamond marker), which is the power limit of the photodiode in the experiment under study. Nevertheless, this BER value being extremely large, a noise floor is definitely expected at higher received powers. To sum, these results confirm the great stability of the QD laser on Si as compared to the QW ones which is a peculiar feature for reflection insensitive transmissions on Si chips. Such a remarkable feedback resistance results from various contributions. First, the low α_H-factor due to the high QD uniformity combined to the very large ES-to-GS lasing threshold preventing the occurrence of the ES emission [13]. Second, the shorter carrier lifetime due to the higher threading dislocation density (TDD) and epitaxial defects hence resulting in a higher damping [17] which can be useful for isolator-free applications but should be somewhat minimized as far as direct modulation of light is concerned.

V. Conclusions

In conclusion, we demonstrate a penalty-free operation with QD lasers on Si operating up to -7.4 dB optical feedback. As opposed to hybrid semiconductor lasers heterogeneously integrated on Si [4], the QD laser under study exhibits a large insensitivity to optical perturbations with 100% of light back reflected to the facet. These results are highly promising for future on-chip reflection insensitive transmitters. Further work will involve direct modulation experiments and investigation of distributed feedback (DFB) lasers. In the latter case, an asymmetric cavity with low (resp. high) reflectivity on the front (resp. rear) facet can indeed alter the feedback sensitivity [18]. Last but not least, the role of the defects on the reflection sensitivity will be analyzed which is of first importance for the development of high performance optoelectronics devices.

References

[1] J. C. Norman, D. Jung, Y. Wan, and J. E. Bowers, "Perspective: The future of quantum dot photonic integrated circuits," *APL Photon.*, vol. 3, no. 3, 2018, Art. no. 030901.

[2] G. Roelkens *et al.*, "III-V/silicon photonics for on-chip and intra-chip optical interconnects," *Laser Photon. Rev.*, vol. 4, no. 6, pp. 751–779, 2010.

[3] G.-H. Duan *et al.*, "Hybrid III–V on silicon lasers for photonic integrated circuits on silicon," *IEEE J. Sel. Topics Quantum Electron.*, vol. 20, no. 4, Jul./Aug. 2014, Art. no. 6100213.

[4] K. Schires, N. Girard, G. Baili, G.-H. Duan, S. Gomez, and F. Grillot, "Dynamics of hybrid III-V silicon semiconductor lasers for integrated photonics," *IEEE J. Sel. Topics Quantum Electron.*, vol. 22, no. 6, pp. 43–49, Nov./Dec. 2016.

[5] G. Eisenstein and D. Bimberg, Eds., *Green Photonics and Electronics*. Cham, Switzerland: Springer, 2017.

[6] K. Mizutani *et al.*, "Isolator free optical I/O core transmitter by using quantum dot laser," in *Proc. IEEE 12th Int. Conf. Group IV Photon. (GFP)*, Aug. 2015, pp. 177–178.

[7] K. Lüdge, Ed., *Nonlinear Laser Dynamics: From Quantum Dots to Cryptography*. Hoboken, NJ, USA: Wiley, 2012.

[8] D. O'Brien *et al.*, "Feedback sensitivity of 1.3 μm InAs/GaAs quantum dot lasers," *Electron. Lett.*, vol. 39, no. 25, pp. 1819–1820, Dec. 2003.

[9] B. Lingnau, W. W. Chow, E. Schöll, and K. Lüdge, "Feedback and injection locking instabilities in quantum-dot lasers: A microscopically based bifurcation analysis," *New J. Phys.*, vol. 15, no. 9, 2013, Art. no. 093031.

[10] C. Otto, B. Globisch, K. Lüdge, E. Schöll, and T. Erneux, "Complex dynamics of semiconductor quantum dot lasers subject to delayed optical feedback," *Int. J. Bifurcation Chaos*, vol. 22, no. 10, 2012, Art. no. 1250246.

[11] L.-C. Lin *et al.*, "Comparison of optical feedback dynamics of InAs/GaAs quantum-dot lasers emitting solely on ground or excited states," *Opt. Lett.*, vol. 43, no. 2, pp. 210–213, Jan. 2018.

[12] H. Huang *et al.*, "Analysis of the optical feedback dynamics in InAs/GaAs quantum dot lasers directly grown on silicon," *J. Opt. Soc. Amer. B, Opt. Phys.*, vol. 35, no. 11, pp. 2780–2787, Nov. 2018.

[13] J. Duan *et al.*, "Semiconductor quantum dot lasers epitaxially grown on silicon with low linewidth enhancement factor," *Appl. Phys. Lett.*, vol. 112, no. 25, Jun. 2018, Art. no. 251111.

[14] D. Jung *et al.*, "High efficiency low threshold current 1.3 μm InAs quantum dot lasers on on-axis (001) GaP/Si," *Appl. Phys. Lett.*, vol. 111, no. 12, Sep. 2017, Art. no. 122107.

[15] F. Grillot, B. Thedrez, J. Py, O. Gauthier-Lafaye, V. Voiriot, and J. L. Lafragette, "2.5-Gb/s transmission characteristics of 1.3-μm DFB lasers with external optical feedback," *IEEE Photon. Technol. Lett.*, vol. 14, no. 1, pp. 101–103, Jan. 2002.

[16] X. Porte, M. C. Soriano, and I. Fischer, "Similarity properties in the dynamics of delayed-feedback semiconductor lasers," *Phys. Rev. A, Gen. Phys.*, vol. 89, no. 2, 2014, Art. no. 023822.

[17] D. Inoue *et al.*, "Directly modulated 1.3 μm quantum dot lasers epitaxially grown on silicon," *Opt. Express*, vol. 26, no. 6, pp. 7022–7033, Mar. 2018.

[18] F. Grillot, "On the effects of an antireflection coating impairment on the sensitivity to optical feedback of AR/HR semiconductor DFB lasers," *IEEE J. Quantum Electron.*, vol. 45, no. 6, pp. 720–729, Jun. 2009.